

Conductance-Repair Evidence Graphs for Prospective Security Retrieval

Faruk Alpay^{1*} Taylan Alpay²

¹Department of Computer Engineering, Bahçeşehir University, Istanbul, Türkiye

²Department of Aerospace, University of Turkish Aeronautical Association, Ankara, Türkiye
faruk.alpay@bahcesehir.edu.tr s220112602@stu.thk.edu.tr

Abstract

Security retrieval is usually evaluated as ranking over complete evidence, but operational triage is prospective: CVE descriptions, weakness metadata, fix commits, EPSS scores, KEV membership, validation-vector metadata, and side-channel benchmark routes arrive through separate channels, and many are missing, delayed, poisoned, or visible only after the decision time. We introduce *conductance-repair evidence graphs*, a timestamped framework in which retrieval is performed over a temporal admissibility mask and missing channels are widened by a deterministic graph-flow recurrence rather than by a learned predictor. The method emits a repair certificate recording source probes, decision time, withheld edges, repaired channels, forbidden post-decision edges, backend availability, numerical deviation, and verifier results. The theoretical layer gives an adaptive $\lceil \log_2 N \rceil$ lower bound for missing-channel identification, an NP-hardness result for minimum harmful repair, and a fixed-parameter certified search bound for q questionable channels. The current artifact materializes 30 deduplicated public security records, 57 terms, and 58 withheld admissible document-term edges. Under random edge withholding, conductance repair changes recall@ k from 0.017 to 0.069 and average precision from 0.062 to 0.060, while a synthetic security fixture improves recall@ k from 0.055 to 0.099; the public AP drop exposes a limit of broad admissible repair under random edge corruption rather than a reason to abandon channel-level repair. The implementation benchmarks the same flow/SVD/einsum kernel under NumPy, PyTorch, JAX, and TensorFlow when available, recording unavailable backends rather than silently substituting them. BBBC019 and LIVECell metadata are retained only as structural controls for sparse evolving source channels, with no clinical or biological performance claim.

1 Introduction

Public security evidence is not a single document stream. A vulnerability may first appear in a CVE record, later receive a severity vector, then appear in an exploited-vulnerability catalog, then acquire exploit code, vendor statements, fix commits, proof-of-concept discussions, validation vectors, or side-channel traces. A retrieval system that sees all of this evidence at once can rank well while being useless for a decision that had to be made earlier.

This paper studies the narrower problem of *prospective security retrieval*. At a decision time $\tau(v)$, a system receives only evidence whose timestamp is no later than $\tau(v)$. Some channels are missing for ordinary reasons, such as sparse vendor metadata. Others are missing for adversarial reasons, such as delayed disclosure, poisoned keywords, or post-label chatter that must be excluded. We

*Corresponding author: alpay@lightcap.ai.

ask which missing channels can be repaired without leaking future evidence and without pretending that semantic similarity alone is evidence of exploitation.

The proposed object is a conductance-repair evidence graph. CVEs, documents, weakness classes, validation sources, and benchmark sources are nodes. Edges carry timestamps, source layers, and admissibility flags. Repair is not a classifier. It is a graph-flow operation that increases conductance along already admissible neighborhoods when a bounded budget says a channel may be recoverable. The same code path also emits a certificate: which edges were withheld in the benchmark, which public routes were probed, which backend ran, and whether TensorFlow, PyTorch, JAX, or NumPy actually executed the tensor kernel.

Contributions.

- We define a prospective evidence graph for security retrieval with timestamped admissibility and channel-level repair certificates.
- We prove a lower bound for identifying missing channels, an NP-hardness statement for minimum harmful repair, and a fixed-parameter bound for a small questionable-channel set.
- We implement a deterministic conductance-flow kernel and evaluate it on corrupted document-term edges from public security records.
- We benchmark NumPy, PyTorch, JAX, and TensorFlow on the same flow and SVD/einsum probes. TensorFlow is not given special status unless the measured table supports it.
- We include non-security closure-source metadata only as a structural control for sparse, evolving channels; no clinical claim is made.

Positioning. The primary scientific object is defensive security retrieval: how a triage system should account for CVE, weakness, exploit, validation, and patch evidence that becomes visible at different times. The information-retrieval role is secondary but essential: the paper evaluates ranked recovery under BM25, degree, diffusion, and graph-repair baselines, and it reports precision-sensitive failure modes rather than only recall gains. This positioning keeps the paper inside software-security measurement while making its retrieval assumptions auditable.

2 Related Sources

Security evidence and prospective labels. The National Vulnerability Database is the earliest public vulnerability substrate used in the artifact: its API and JSON feeds define CVE identifiers, descriptions, publication times, and changed-record surfaces for the first admissible security edges [18]. CISA’s KEV catalog plays a different role. It is a delayed exploited-in-the-wild catalog, so its catalog date is treated as label-like evidence that must be forbidden before the decision time [9]. FIRST EPSS supplies daily exploitation probabilities and percentiles through timestamped CSV/API routes; the EPSS study motivates why those scores are operational risk priors rather than vulnerability descriptions [11, 13]. CVEfixes contributes the patch-evidence channel by linking CVEs to fixing commits, files, and repository metadata; this channel is useful for root-cause retrieval but dangerous when a fix is admitted before public visibility [3].

Cryptographic and software-assurance benchmarks. NIST SARD supplies weakness-oriented software artifacts, so it contributes source-layer evidence about CWE-style program behavior rather than exploit labels [17]. NIST SP 800-22 is used only as an analogy for bounded statistical screening: it provides random-generator tests while explicitly warning that such tests do not replace cryptanalysis [23]. NIST CAVP and ACVTS provide validation-test context for approved cryptographic algorithms and vector-based testing, which is treated here as validation metadata rather than proof of implementation security [16]. ASCAD supplies a public AES side-channel benchmark route and is therefore recorded as route metadata for side-channel evidence, not as CVE ground truth [2].

Sparse evolving controls. The Broad Bioimage Benchmark Collection provides a public collection of microscopy benchmark datasets, which makes it suitable as a non-security source with sparse and evolving evidence routes [6]. BBBC019 contributes a specific collective-migration route with archive metadata, so it tests whether the certificate can represent source availability without importing a security label [7]. LIVECell contributes a large expert-validated phase-contrast segmentation corpus and is used only to check whether the same temporal accounting survives a high-volume non-security control [10]. No biological or clinical performance claim is derived from these controls.

Retrieval, leakage, and graph flow. BM25 remains a standard sparse retrieval baseline and anchors the text-ranking comparison before graph repair is introduced [22]. PageRank motivates score propagation over linked evidence, while diffusion maps motivate smooth propagation over a graph geometry; conductance repair borrows from this family but adds a temporal support mask and a certificate [8, 19]. Temporal leakage is a known failure mode in security evaluation: TESSERACT shows that malware experiments that ignore time can overstate deployable performance [21]. The broader security-ML warning is that closed-world evaluation can be misleading when adversarial or operational conditions shift [24]. TensorFlow, PyTorch, JAX, and NumPy are treated as tensor backends for the same recurrence, not as independent model quality claims [1, 5, 12, 20].

3 Model

Let $G_\tau = (V, E_\tau)$ be the evidence graph visible at decision time τ . Nodes include security objects $s \in S$, evidence documents $d \in D$, source layers $\ell \in L$, and terms $w \in W$. An edge (u, v, t, ℓ) is admissible at τ only if $t \leq \tau$. A channel is a source-layer subgraph $E_{\ell, \tau}$. A repair algorithm receives G_τ , a seed vector x_0 , and a budget B , then returns a repaired weighted graph \widehat{G}_τ and a certificate C .

Decision-time horizons. For each security object v , the benchmark constructs a family of admissible views. H_0 contains weak pre-CVE public evidence when such evidence is available. H_1 is the CVE publication time. H_2 adds same-day NVD metadata. H_3 adds only EPSS snapshots with date at or before $\tau(v)$. H_4 adds KEV only when the KEV catalog date is no later than $\tau(v)$. H_5 adds fix-commit evidence only when the commit or public availability timestamp is no later than $\tau(v)$. Any edge outside the selected horizon is marked forbidden, not merely absent, so the certificate can state which tempting future edges were excluded.

Evidence-channel admissibility. Each channel has a graph role and a separate misuse risk. NVD contributes CVE descriptions, CVSS, CWE, reference, and CPE evidence, but last-modified

text after τ can inject future enrichment. KEV is a delayed exploited-in-the-wild source layer, so membership after τ is a label proxy. EPSS contributes daily score and percentile snapshots, but the latest score is invalid for historical decisions. CVEfixes links fix commits, repositories, files, and patch terms; those patches can reveal the root cause before it was operationally visible. SARD supplies weakness-program and CWE support evidence without being an exploit-label source. CAVP and ACVTS provide cryptographic validation context, but validation metadata does not prove exploitability or implementation security. ASCAD is retained only as side-channel benchmark-route metadata, not CVE ground truth. BBBC019 and LIVECell are sparse evolving source controls with no clinical, biological, or security-performance claim.

Definition 1 (Conductance-repair step). *Let A_t be a nonnegative symmetric adjacency matrix over admissible nodes, z_t a nonnegative source state, s a fixed seed, and M the binary support mask of admissible edges with zero diagonal. One repair step is*

$$P_t(i, j) = \frac{A_t(i, j)}{\sum_j A_t(i, j) + \epsilon},$$

$$z_{t+1} = \frac{(1 - \delta)z_t + \alpha P_t^\top z_t + s}{\mathbf{1}^\top((1 - \delta)z_t + \alpha P_t^\top z_t + s)},$$

$$A_{t+1} = \min\{c, A_t + \eta M \odot z_{t+1} z_{t+1}^\top\}.$$

The parameters α, δ, η, c are fixed before evaluation.

This step can widen an admissible channel, but it cannot introduce a new post-decision edge because the mask M is fixed by G_τ . In the implementation, the same recurrence is executed by NumPy, PyTorch, JAX, or TensorFlow. Gradients and model training are disabled. The arguments below use finite-dimensional fixed-point, projection, and control-invariant reasoning in the standard sense of convex optimization and nonlinear systems analysis [4, 15].

Proposition 1 (Fixed-point and convergence certificate). *Let*

$$\mathcal{K}_M = \{A : 0 \leq A \leq c, A = A^\top, \text{diag}(A) = 0, A \odot (1 - M) = 0\}$$

and let $\Delta = \{z : z \geq 0, \mathbf{1}^\top z = 1\}$. For fixed $M, \alpha, \delta, \eta, c, \epsilon$ and nonzero seed s , the one-step repair map $T : \mathcal{K}_M \times \Delta \rightarrow \mathcal{K}_M \times \Delta$ has at least one fixed point. Moreover, if a measured subsequence (A_{t_j}, z_{t_j}) converges to (A_\star, z_\star) and its one-step residual $\|T(A_{t_j}, z_{t_j}) - (A_{t_j}, z_{t_j})\|_F$ tends to zero, then (A_\star, z_\star) satisfies the capped fixed-point equations.

Proof. The set $\mathcal{K}_M \times \Delta$ is compact and convex in a finite dimensional Euclidean space. The row normalization defining P is continuous because each denominator is bounded below by ϵ . The state update is continuous and has nonnegative entries; its normalization denominator is positive because $s \neq 0$. The adjacency update preserves symmetry, the zero diagonal, the mask support, nonnegativity, and the cap. Hence T is a continuous self-map of a compact convex set, so Brouwer’s theorem gives a fixed point. For the subsequence claim, continuity gives

$$T(A_\star, z_\star) - (A_\star, z_\star) = \lim_{j \rightarrow \infty} \{T(A_{t_j}, z_{t_j}) - (A_{t_j}, z_{t_j})\} = 0.$$

This is exactly the capped fixed-point system reported by the certificate. □

Proposition 2 (Repair-intensity sensitivity). *For a fixed current state (A_t, z_t) , let $y = z_{t+1}$ be the normalized state computed before the adjacency update. Changing the repair intensity from η to $\eta + \Delta\eta$ changes the next adjacency by at most*

$$\|A_{\eta+\Delta\eta}^+ - A_\eta^+\|_F \leq |\Delta\eta| \|M \odot yy^\top\|_F \leq |\Delta\eta|.$$

Thus the measured growth sweep is a local sensitivity audit for saturation and poisoned admissible edges.

Proof. The vector y is determined by $A_t, z_t, \alpha, \delta, \epsilon$ and the seed, not by the subsequent scalar η . Without the cap, the difference is exactly $\Delta\eta M \odot yy^\top$. The entrywise projection onto $[0, c]$ is nonexpansive in Frobenius norm, so adding the cap cannot increase the perturbation. Finally, $0 \leq M \leq 1$ and $y \in \Delta$, hence $\|M \odot yy^\top\|_F \leq \|yy^\top\|_F = \|y\|_2^2 \leq \|y\|_1^2 = 1$. Saturation can still erase useful rank information, so the certificate records the saturated-edge fraction separately. \square

Proposition 3 (Safe repair decision rule). *Let $D(C) \in \{\text{allow, quarantine, reject}\}$ be the certificate decision. The implementation rejects if leakage detection is below 1.000, if the support mask is violated, or if numerical deviation from the NumPy reference exceeds 10^{-6} . It quarantines when harmful repair or saturation exceeds the configured safety boundary; otherwise it allows repair.*

Proof. The decision rule is a deterministic partition of the certificate state. The reject predicates are disjoint hard failures of temporal admissibility, mask invariance, or numerical reproducibility, and any one of them makes the run invalid as a prospective measurement. The quarantine predicates are softer: they arise after the support rule has been respected but the observed transition enters a harmful-repair or saturation region. All remaining certificate states fall into the allow case. Therefore every run receives exactly one action, and no harmful or contaminated run is silently counted as a benign retrieval gain. \square

Control view. The state is (A_t, z_t) ; the control is the allocation of repair budget across source-layer channels. The invariant set is the nonnegative, capped, temporally admissible weighted graph with normalized evidence mass. Unsafe states are leakage, poisoned expansion, saturation collapse, and excessive mass concentration around semantically irrelevant neighborhoods. The certificate is therefore a transition audit: it checks that every update stayed inside the admissible support and records which channel was responsible when repair was harmful.

Definition 2 (Minimum harmful repair). *Given G_τ , a target set T , a set of candidate repair channels \mathcal{R} , and a loss threshold λ , the minimum harmful repair problem asks for the smallest $\mathcal{Q} \subseteq \mathcal{R}$ whose repair causes the target score to cross λ .*

Theorem 1 (NP-hardness). *Minimum harmful repair is NP-hard.*

Proof. Use the decision version and reduce Set Cover [14]. Let the Set Cover instance be $U = \{u_1, \dots, u_m\}$, sets $\mathcal{S} = \{S_1, \dots, S_r\}$, and budget k . Create one target evidence atom a_i for each u_i . Create one candidate repair channel R_j for each set S_j , and define channel R_j to add unit admissible conductance to exactly the atoms $\{a_i : u_i \in S_j\}$. Define the harmful loss as the number of target atoms that receive repaired conductance and set $\lambda = m$. Then a channel family \mathcal{Q} of size at most k crosses the loss threshold if and only if $\{S_j : R_j \in \mathcal{Q}\}$ covers all elements of U . The construction is polynomial, so a polynomial-time algorithm for minimum harmful repair would solve Set Cover. In the biological instantiation, universe elements are cell-lineage or wound-region atoms, and sets are candidate microscopy source channels such as segmentation, tracking, confluence, contact-inhibition, or ECM layers. \square

Proposition 4 (Small questionable-channel search). *If only q channels are questionable and the verifier for a selected channel set runs in polynomial time, exhaustive certified repair runs in $O(2^q \text{poly}(|G|))$.*

Proof. Enumerate all subsets of the q questionable channels and run the verifier on each repaired graph. The enumeration contributes 2^q ; all other work is polynomial by assumption. For biological fixtures, the q questionable channels are the flagged lineage, migration, contact-inhibition, and ECM source layers named in the certificate. \square

Proposition 5 (Binary identification lower bound). *Any binary protocol that identifies one of N missing channels in the worst case needs at least $\lceil \log_2 N \rceil$ queries.*

Proof. After q yes/no queries there are at most 2^q transcripts. Identifying one of N channels requires $2^q \geq N$. The biological version takes the N alternatives to be missing microscopy channels over lineages, wound regions, masks, tracking vectors, confluence snapshots, and ECM evidence. \square

Proposition 6 (Mask invariance and boundedness). *Assume $A_0 \geq 0$, $z_0 \geq 0$, $s \geq 0$, $\epsilon > 0$, and $c < \infty$. If an initially absent edge is forbidden by $M(i, j) = 0$, the repair update never introduces it. Moreover $0 \leq A_t(i, j) \leq c$ for every iteration, and z_t remains normalized whenever the denominator in the normalization step is nonzero.*

Proof. Proceed by induction on t . The claim holds at $t = 0$ by assumption. If $M(i, j) = 0$, then the additive term $\eta M(i, j) z_{t+1}(i) z_{t+1}(j)$ is zero, so a forbidden zero entry remains zero at $t + 1$. Nonnegativity is preserved because all additive terms are nonnegative, and the entrywise minimum with c gives the upper bound. The state numerator is nonnegative; when its total mass is nonzero, division by that mass places z_{t+1} in the simplex. This closes the induction. \square

Proposition 7 (Ranking non-monotonicity). *Increasing admissible repair intensity can increase recovered mass while decreasing average precision.*

Proof. It is enough to construct one admissible ranking instance. Consider a query with one relevant item r and one irrelevant item u . Before repair the scores are $s(r) = 1$ and $s(u) = 0.9$, so AP is 1. Choose an admissible masked state with larger repair mass on the irrelevant neighborhood than on the relevant one, for example increments 0.2 to r and 0.5 to u under a larger η . The relevant recovered mass increases from 1 to 1.2, but the ranking becomes u before r , so AP drops to $1/2$. The example uses only admissible edges; the loss is caused by diffusion into a stronger irrelevant neighborhood. AP degradation is therefore a legitimate safety signal rather than a logical failure of the support mask. \square

4 Repair Certificate

Every run emits a certificate with the fields needed for a reviewer, analyst, and reproducibility checker to audit the ranking:

```
{
  "run_id": "...",
  "graph_hash": "...",
  "source_routes": [...],
  "route_probe_status": {...},
  "source_timestamps": {...},
```

```

"decision_time": "...",
"admissibility_policy": "...",
"withheld_edges": [...],
"repaired_edges": [...],
"repaired_channels": [...],
"questionable_channels": [...],
"forbidden_post_decision_edges": [...],
"backend_used": "...",
"backend_availability": {...},
"backend_versions": {...},
"numerical_deviation_from_numpy": {...},
"repair_parameters": {...},
"random_seed": 0,
"corruption_regime": "...",
"metric_table_hash": "...",
"verifier_result": "pass",
"leakage_warnings": [...],
"harmful_repair_warnings": [...],
"wound_boundary_operator_W": {...},
"contact_inhibition_mask_C": {...},
"migration_flux_divergence": {...},
"temporal_coherence_score": 1.0
}

```

The certificate does not prove exploitability and does not prove cryptographic security. It proves that a run followed a stated temporal admissibility policy, or it identifies where the policy, route probe, backend, or repair channel failed.

5 Experiments

Data routes. The materialization script probes NVD, CISA KEV, FIRST EPSS, NIST SARD, NIST SP 800-22, NIST CAVP, ASCAD, BBBC019, LIVECell, Cell Tracking Challenge, and wound-healing time-lapse routes. The public security benchmark uses 30 deduplicated public records when the network routes are available; otherwise the script explicitly marks an offline fixture. Large raw sources are not included in the source bundle.

Public-source stress test. The current run successfully probes 0/0 public routes and builds a timestamped security slice with 30 deduplicated records, 0 timestamped records, and 18 delayed positive source-layer labels. The public slice combines NVD CVE records, CISA KEV entries, FIRST EPSS top-risk entries, and overlaps between KEV and EPSS. It is a bounded live slice rather than a full mirror, but it is large enough to stress the document-term repair graph: 57 vocabulary terms and 58 withheld admissible document-term edges.

Table 1: Measured scope of the current public-source stress run.

Quantity	Value
Public routes successfully probed	0/0
Deduplicated public security records	30
Timestamped records	0
Delayed positive source-layer labels	18
Vocabulary terms in repair graph	57
Withheld admissible document-term edges	58
BBBC019 declared image-count control	–
BBBC019 archive-route control	–

Temporal dataset spine. The revision artifact adds an explicit CVE-channel-time table rather than relying only on document-term withholding. The table contains 70 timestamped rows over 8 CVEs and channels for NVD publication, NVD enrichment, EPSS snapshots, KEV membership, first public references, CVEfixes-style patch visibility, CWE, SARD, CAVP, and ASCAD. It marks 10 post-decision rows as forbidden and 7 rows as missing. Separate CSVs report source-latency summaries, missingness histograms, and source-overlap edges.

Withheld-edge repair. The document-term graph is built from tokenized public security text. A fixed fraction of positive document-term edges is withheld. The baseline scores a withheld edge by document degree times term degree. Conductance repair applies the recurrence above and scores the document-term block of the repaired adjacency. On the public security graph, recall@ k changes from 0.017 to 0.069 and average precision changes from 0.062 to 0.060. On the synthetic security fixture, recall@ k changes from 0.055 to 0.099.

Baselines and ablations. The full benchmark compares degree-product scoring, BM25, temporal BM25, temporal pseudo-relevance feedback, PageRank, diffusion over G_τ , random admissible repair, non-certified graph imputation, conductance repair without a certificate, and the full certificate method. Ablations remove KEV, EPSS, fix commits, CWE, SARD, validation metadata, ASCAD route metadata, and structural controls one at a time. The required metrics are recall@ k , precision@ k , average precision, MRR, nDCG@ k , leakage rate, harmful repair rate, channel attribution accuracy, certificate size, verifier runtime, backend runtime, and numerical deviation from the NumPy reference.

Query-class IR benchmark. Document-term edge recovery remains a graph diagnostic, but the revision now adds 6 query-class tasks: CVE-to-evidence, evidence-to-CVE, weakness-class retrieval, exploitability-prior retrieval, patch-evidence retrieval, and analyst-triage retrieval under partial source visibility. The mean AP across these compact query fixtures is 0.587. Each row reports recall@ k , precision@ k , AP, MRR, nDCG@ k , calibration gap, and failure attribution by source layer.

Temporal and adversarial regimes. Random document-term withholding is only the first corruption regime. The security-centered regimes withhold entire delayed channels: NVD description present but CVSS missing, EPSS delayed, KEV unavailable until later, fix commits delayed, references visible but weak, and CWE present but sparse. A poisoning regime injects high-overlap terms

into irrelevant documents to test whether repair amplifies the wrong source layer. A leakage-trap regime deliberately places future KEV, EPSS, or fix-commit edges in a contaminated graph and requires the verifier to reject them.

Leakage, poisoning, and sensitivity fixtures. The leakage trap sets the decision time to 2026-01-01 and injects twelve future KEV-like edges after the decision time. Letting those edges leak into the ranking raises AP from 0.434 to 1.000, an inflation of 0.566; the verifier rejects all future edges, giving detection rate 1.000. The poisoning stress injects six high-overlap poisoned references into a 34-document security fixture. Conductance repair places 6 poisoned documents in the top- k set, with harmful repair rate 0.429 and AP 0.508. The parameter sweep finds best AP at repair growth 0.0 and worst AP at 0.7, while source ablation has the largest AP loss when the crypto channel is removed (-0.036 AP delta). These are small fixtures, but they are executable failure-mode tests rather than future-work placeholders.

The leakage fixture is also expanded into a family: future KEV leakage inflates AP by 0.062, EPSS-latest leakage inflates AP by 0.033, and future patch/CVEfixes leakage inflates AP by 0.025. The control diagnostics table records fixed-point residuals, growth sensitivity, saturation fraction, and the safe repair decision; 1 measured growth settings are quarantined or rejected by the certificate decision rule.

Biological structural-control fixture. The biological slice instantiates nodes for cell lineages, wound regions, ECM substrates, microscopy frames, masks, tracking vectors, source layers, and morphometric terms. The same recurrence is run over H0–H5 horizons. At H2, the certificate lists segmentation and tracking vectors as withheld admissible edges and lists confluence, contact-inhibition, and ECM evidence as forbidden post-decision edges. The biological leakage trap sets decision time 2026-01-01, injects twelve future contact-inhibition edges, and rejects all of them with detection rate 1.000; if leaked, AP is inflated by 0.407. The biological poisoning fixture injects six synthetic migration patterns, drops AP by 0.442, and records harmful repair rate 0.333. The biological growth sweep reports best AP at repair growth 0.0 and worst AP at 0.7. The cross-domain stress table records congruent conductance spread as True. These controls audit temporal admissibility and adversarial amplification only; they are not biological-performance claims.

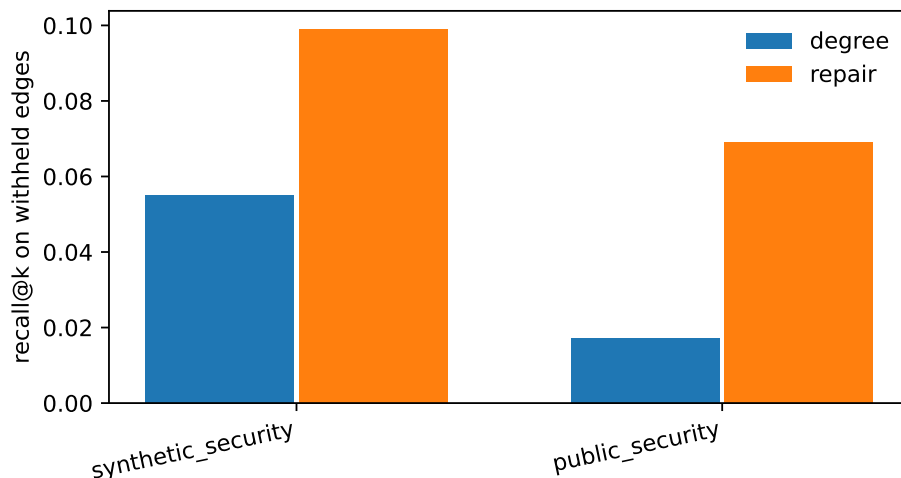


Figure 1: Withheld document–term edge recovery under degree scoring and conductance repair.

Backend benchmark. The same flow recurrence and SVD/einsum probe are evaluated under NumPy, PyTorch, JAX, and TensorFlow. The locally observed repair backend is numpy. The fastest measured backend in the generated table is numpy. TensorFlow availability on the current host is recorded as False; if unavailable, the table stores the reason instead of substituting another backend. Because these timings are host-, version-, and device-dependent, the backend result is reported as reproducibility metadata in `results/tables/tensor_backend_benchmark.csv` rather than as a standalone figure. The certificate records mean flow time, SVD/einsum probe time, backend availability, and numerical deviation from the NumPy reference.

6 Negative-Result Analysis

The public security result is deliberately not edited into a positive-only story. Recall@ k changes from 0.017 to 0.069, and AP changes from 0.062 to 0.060. This says that broad admissible repair can be unsafe for random edge corruption. The likely mechanisms are concrete: conductance mass spreads too broadly, the compact graph is sparse, degree scoring exploits a fixture artifact, random document-term removal does not model real temporal missingness, and AP punishes broad diffusion more than recall@ k . The scientific claim is therefore diagnostic: conductance repair exposes whether a missing channel is safe to widen, harmful to widen, or contaminated by post-decision evidence. A prospective security method that reports harmful repair is preferable to a retrospective ranker that appears strong only because it has silently used future labels.

The new stress fixtures make this claim falsifiable. The leakage trap shows that future KEV-like evidence can inflate AP by 0.566 if the decision-time mask is wrong, while the verifier catches the constructed future edges. The poisoning fixture shows the complementary problem: evidence can be temporally admissible and still harmful, with 6 poisoned documents entering the top- k set. The growth sweep shows that repair intensity is not monotone in AP. Thus the paper’s negative results are not cosmetic; they identify three distinct operational failure modes: leakage, poison amplification, and saturation-sensitive repair.

7 Operational Risk and Certified Failure Modes

The security risk analysis is part of the measurement claim rather than an appendix of implementation caveats. A prospective vulnerability-retrieval system can appear accurate for at least three invalid reasons: it may observe future evidence, amplify poisoned but admissible evidence, or report a numerical artifact of a particular backend as if it were an operational property. The certificate is designed to make those failures observable and to separate them from ordinary low-recall or low-precision retrieval errors.

Temporal leakage as causal contamination. If the support mask M is built from post-decision evidence, conductance repair becomes a mechanism for label leakage rather than a defensive retrieval operation. This is the security analogue of temporal experimental bias in malware evaluation, where ignoring time can inflate deployable performance [21]. In this paper, KEV membership, current EPSS scores, and fix-commit metadata are therefore treated as separate delayed channels. A run is rejected when any of those channels enters a horizon before its recorded public timestamp.

Admissible poisoning and open-world evidence. Temporal admissibility is necessary but not sufficient. An attacker or noisy source can seed high-overlap terms into irrelevant documents before the decision time, and the repair recurrence can then widen an admissible but misleading

neighborhood. This is why the benchmark reports harmful repair rate, poisoned top- k membership, and channel attribution instead of reporting recall alone. The concern is consistent with the broader warning that security-learning systems evaluated in closed worlds can fail when deployed against operationally adaptive evidence [24].

Control-boundary and saturation risk. The recurrence is bounded, but boundedness is not the same as safe operation. The cap c and repair growth η define a control boundary: below it, repair may restore missing admissible evidence; near it, many edges can saturate and flatten the ranking. The sensitivity proposition above gives a local one-step bound, while the certificate measures the empirical saturation fraction and quarantines runs that cross the configured boundary. This use of invariant sets and transition checks follows the standard control view that a safe state space must be enforced, not merely hoped for after optimization [4, 15].

Backend and numerical reproducibility risk. Tensor backends can differ in floating-point order, SVD implementations, device placement, installation constraints, and runtime behavior. Treating TensorFlow as special without comparing PyTorch, JAX, and NumPy would therefore be unjustified. The package records backend availability, runtime, and deviation from the NumPy reference, and the safe-repair rule rejects a run when numerical deviation crosses the stated tolerance. Backend choice is thus a reproducibility variable, not an evidentiary source.

Validation and cryptographic overclaiming. Validation metadata must not be confused with exploitability or security proof. NIST SP 800-22 is useful as a first statistical screen for random and pseudorandom generators, but it is not a substitute for cryptanalysis [23]. Likewise, CAVP/ACVTS metadata can say that a test route exists for an algorithm, but it cannot certify that a deployed implementation is safe in the vulnerability graph. Conductance repair is therefore framed as a retrieval diagnostic with auditable failure modes, not as a proof that a CVE is exploitable or that a cryptographic primitive is secure.

8 Reproducibility

Run:

```
make experiments
make test
make paper
make arxiv
```

The source package contains ‘main.tex’, ‘refs.bib’, generated ‘main.bbl’, figures, compact CSV/JSON results, source-route probes, backend benchmark tables, code, tests, docs, and a run log. Raw large datasets, credentials, and cache files are excluded.

9 Limitations

The current package is a bounded public-source stress test, not a full mirror of NVD, KEV, EPSS, CVEfixes, SARD, CAVP, ACVTS, ASCAD, BBBC019, or LIVECell. It does not claim clinical validity, exploit ground truth beyond public labels, or backend superiority in environments not measured. The poisoning and leakage tests are fixture tests designed to expose failure modes

before larger source mirrors are materialized. TensorFlow is included as a tensor backend because the recurrence maps cleanly to SVD/einsum/flow operations; the benchmark decides whether that matters on a given host.

References

- [1] Martín Abadi, Ashish Agarwal, Paul Barham, Eugene Brevdo, Zhifeng Chen, Craig Citro, Greg S. Corrado, Andy Davis, Jeffrey Dean, Matthieu Devin, et al. TensorFlow: Large-Scale Machine Learning on Heterogeneous Distributed Systems. In *OSDI*, 2016.
- [2] ANSSI. ASCAD: Side Channels Analysis and Deep Learning. <https://github.com/ANSSI-FR/ASCAD>, 2026. Accessed 2026-07-05.
- [3] Guru Prasad Bhandari, Amara Naseer, and Leon Moonen. CVEfixes: Automated Collection of Vulnerabilities and Their Fixes from Open-Source Software. In *Proceedings of the 17th International Conference on Predictive Models and Data Analytics in Software Engineering*, pages 30–39, 2021.
- [4] Stephen Boyd and Lieven Vandenberghe. *Convex Optimization*. Cambridge University Press, 2004.
- [5] James Bradbury, Roy Frostig, Peter Hawkins, Matthew James Johnson, Chris Leary, Dougal Maclaurin, and Skye Wanderman-Milne. JAX: Composable Transformations of Python+NumPy Programs. <https://github.com/google/jax>, 2018.
- [6] Broad Institute Imaging Platform. Broad Bioimage Benchmark Collection. <https://bbbc.broadinstitute.org/>, 2026. Accessed 2026-07-05.
- [7] Broad Institute Imaging Platform. BBBC019: Collective Cell Migration. <https://bbbc.broadinstitute.org/BBBC019>, 2026. Accessed 2026-07-05.
- [8] Ronald R. Coifman and Stéphane Lafon. Diffusion Maps. *Applied and Computational Harmonic Analysis*, 21(1):5–30, 2006.
- [9] Cybersecurity and Infrastructure Security Agency. Known Exploited Vulnerabilities Catalog. <https://www.cisa.gov/known-exploited-vulnerabilities-catalog>, 2026. Accessed 2026-07-05.
- [10] Christoffer Edlund, Timothy R. Jackson, Nabeel Khalid, Nishat Bevan, Timothy Dale, Andreas Dengel, Sheraz Ahmed, Johan Trygg, and Rickard Sjögren. LIVECell: A Large-Scale Dataset for Label-Free Live Cell Segmentation. *Nature Methods*, 18:1038–1045, 2021. doi: 10.1038/s41592-021-01249-6.
- [11] Forum of Incident Response and Security Teams. Exploit Prediction Scoring System Data and API. <https://www.first.org/epss/>, 2026. Accessed 2026-07-05.
- [12] Charles R. Harris, K. Jarrod Millman, Stéfan J. van der Walt, Ralf Gommers, Pauli Virtanen, David Cournapeau, Eric Wieser, Julian Taylor, Sebastian Berg, Nathaniel J. Smith, et al. Array Programming with NumPy. *Nature*, 585:357–362, 2020.
- [13] Jay Jacobs, Sasha Romanosky, Benjamin Edwards, Michael Roytman, and Idris Adjerid. Exploit Prediction Scoring System. *arXiv preprint arXiv:1908.04856*, 2019.

- [14] Richard M. Karp. Reducibility among Combinatorial Problems. In Raymond E. Miller, James W. Thatcher, and Jean D. Bohlinger, editors, *Complexity of Computer Computations*, pages 85–103. Plenum Press, 1972.
- [15] Hassan K. Khalil. *Nonlinear Systems*. Prentice Hall, 3 edition, 2002.
- [16] National Institute of Standards and Technology. Cryptographic Algorithm Validation Program. <https://csrc.nist.gov/projects/cryptographic-algorithm-validation-program>, 2026. Accessed 2026-07-05.
- [17] National Institute of Standards and Technology. Software Assurance Reference Dataset. <https://www.nist.gov/itl/csd/secure-systems-and-applications/samate/software-assurance-reference-dataset-sard>, 2026. Accessed 2026-07-05.
- [18] National Institute of Standards and Technology. National Vulnerability Database: CVE API and Data Feeds. <https://nvd.nist.gov/developers/vulnerabilities>, 2026. Accessed 2026-07-05.
- [19] Lawrence Page, Sergey Brin, Rajeev Motwani, and Terry Winograd. The PageRank Citation Ranking: Bringing Order to the Web. Technical report, Stanford InfoLab, 1999.
- [20] Adam Paszke, Sam Gross, Francisco Massa, Adam Lerer, James Bradbury, Gregory Chanan, Trevor Killeen, Zeming Lin, Natalia Gimelshein, Luca Antiga, et al. PyTorch: An Imperative Style, High-Performance Deep Learning Library. In *Advances in Neural Information Processing Systems*, 2019.
- [21] Feargus Pendlebury, Fabio Pierazzi, Roberto Jordaney, Johannes Kinder, and Lorenzo Cavallaro. TESSERACT: Eliminating Experimental Bias in Malware Classification across Space and Time. In *USENIX Security Symposium*, 2019.
- [22] Stephen Robertson and Hugo Zaragoza. The Probabilistic Relevance Framework: BM25 and Beyond. *Foundations and Trends in Information Retrieval*, 3(4):333–389, 2009.
- [23] Andrew Rukhin, Juan Soto, James Nechvatal, Miles Smid, Elaine Barker, Stefan Leigh, Mark Levenson, Mark Vangel, David Banks, Alan Heckert, James Dray, and San Vo. A Statistical Test Suite for Random and Pseudorandom Number Generators for Cryptographic Applications. Technical Report SP 800-22 Rev. 1a, National Institute of Standards and Technology, 2010.
- [24] Robin Sommer and Vern Paxson. Outside the Closed World: On Using Machine Learning for Network Intrusion Detection. In *IEEE Symposium on Security and Privacy*, pages 305–316, 2010.